KLF5-induced miR-487a augments the progression of osteosarcoma cells by targeting NKX3-1 *in vitro*

ANYU LUO, HANLIN LIU and CHEN HUANG

Department of Orthopedics, Hanyang Hospital Affiliated to Wuhan University of Science and Technology, Wuhan, Hubei 430051, P.R. China

Received June 2, 2021; Accepted May 10, 2022

DOI: 10.3892/ol.2022.13378

Abstract. MicroRNAs (miRNAs or miRs) are involved in the development and progression of numerous types of cancer however their role in osteosarcoma has not been fully clarified. The present study aimed to use high-throughput bioinformatics analysis as well as *in vitro* experiments to investigate the potential role of transcription factors, miRNAs and their targets in the progression of osteosarcoma. miRNA data and clinical information of osteosarcoma were obtained from Gene Expression Omnibus database to investigate differentially expressed miRNAs. The expression of miRNAs/mRNAs in osteosarcoma cell lines was detected via reverse transcription-quantitative (RT-qPCR). MTT and colony formation assay were used to determine cell proliferation ability and transwell assay was used to observe cell invasion and migration ability. A total of four prediction algorithms for miRNA-mRNA interactions were used to determine potential target genes of miR-487a. Predicted target genes were used to intersect with overlapped differentially expressed genes (DEGs) from GSE12865 and The Cancer Genome Atlas osteosarcoma datasets. Expression of NK3 homeobox 1 (NKX3-1) was analyzed by western blotting and RT-qPCR assay. Dual luciferase assay was conducted to verify whether NKX3-1 was a direct target of miR-487a. The regulatory association between Kruppel-like factor 5 (KLF5) and miR-487a was detected using chromatin immunoprecipitation assay. miR-487a was upregulated in osteosarcoma tissue (GSE65071 and GSE28423) and cell lines (HOS and MG63). miR-487a mimic promoted proliferation, migration and invasion of osteosarcoma cells. NKX3-1 was a direct target of miR-487a and transfection of NKX3-1 plasmid reversed the effect of miR-487a on proliferation, migration and invasion of osteosarcoma cells. KLF5 enhanced miR-487a expression by directly binding to its promoter region and miR-487a inhibitor reversed the effect of KLF5 on proliferation, migration and invasion of osteosarcoma cells. The present results indicated that KLF5/miR-487a signaling promoted invasion and metastasis of osteosarcoma cells via targeting NKX3-1.

Correspondence to: Dr Chen Huang, Department of Orthopedics, Hanyang Hospital Affiliated to Wuhan University of Science and Technology, 53 Moshuihu Road, Hanyang, Wuhan, Hubei 430051, P.R. China
E-mail: zxdwuhan@163.com

Key words: microRNA-487a, NK3 homeobox 1, osteosarcoma, Kruppel-like factor 5, The Cancer Genome Atlas, Gene Expression Omnibus

Introduction

Osteosarcoma is a common, highly malignant bone tumor which has high metastatic potential, occurring mainly in children and adolescents (1). Osteosarcoma mainly occurs in the proximal tibia or distal femur and is highly malignant and prone to invasion and metastasis (2,3). In spite of the use of neoadjuvant chemotherapy (4), the 5-year survival rate of patients osteosarcoma with metastasis or recurrence is poor (5). Thus, investigating the pathogenesis of osteosarcoma may lead to development of novel therapeutic targets.

MicroRNAs (miRNAs or miRs) are a class of single-stranded, non-coding small RNA that regulate gene expression by binding to the 3' untranslated region (3'-UTR) of target genes (6,7). miRNAs have been reported to be associated with biological processes including cell proliferation, migration and inflammation, as well as apoptosis (8,9). In addition, miRNAs serve as oncogenes or cancer suppressors, which serves a key role in tumorigenesis (10-12). Numerous studies have demonstrated that miRNAs modulate the progression of osteosarcoma (13,14). Studies have revealed the effect of miR-487a on cancer. For example, Yang *et al* (15) demonstrated that miR-487a promotes progression of gastric cancer by targeting TIA1. Ma *et al* (16) indicated that miR-487a enhances TGF-β1-induced epithelial-mesenchymal transition, migration and invasion of breast cancer cells via directly targeting membrane-associated guanylate kinase, WW and PDZ domain-containing 2. Several studies have shown that transcription factors and miRNAs are involved in the development of cancer (17,18). However, the precise mechanism of TF-miR-487a in the progression of osteosarcoma remained to be fully explored.

The present study investigated candidate molecules that may play important roles in the occurrence and development of osteosarcoma through bioinformatics screening and experimental verification, and finally identified that

the KLF5/miR-487a/NKX3-1 axis plays an important role in the proliferation, invasion and metastasis of osteosarcoma, which may offer aid to find new therapeutic targets for osteosarcoma.

Materials and methods

Bioinformatics analysis. miRNA data and clinical information of osteosarcoma were obtained from Gene Expression Omnibus (GEO; ncbi.nlm.nih.gov/geo/) database (accession nos. GSE65071 and GSE28423; Table SI). DESeq2 package (Version 3.12) (19) was used to normalize raw osteosarcoma miRNAs and identify differentially expressed miRNAs (DEMs) between the osteosarcoma and non-osteosarcoma samples/cells. P<0.01 and logFC >4 were considered to indicate a statistically significant difference. Osteosarcoma DEMs were obtained by overlapping DEMs from GSE65071 with DEMs from GSE28423 dataset. Overlapped miRNAs were observed using vennDiagram (Version: 1.6.20; cran.r-project.org/src/contrib/Archive/VennDiagram/) package. Volcano map was constructed using ggplot2 package (Version: 3.3.2; cran.r-project.org/src/contrib/Archive/ggplot2/) to measure and analyze DEMs.

Prediction of miR-487a target genes and promoter binding sites. JASPAR database was used to determine candidate transcription factors targeting promoters of miR-487a (20). The predicted binding ability was ranked based on binding score. Online prediction software miRWalk2.0 (21), TargetScan 6.2 (22), miRanda 1.0 (23) and RNA22 2.0 (24) were used to determine potential target genes of miR-487a. Predicted target genes were overlapped with DEGs of GSE12865 and TARGET-OS (ocg.cancer.gov/programs/target/projects/osteosarcoma) sets (Table SI). DEGs between osteosarcoma tissue and non-osteosarcoma controls were identified as previously described (19). PCR and western blot assay were used to verify results.

Cell culture and transfection. Osteosarcoma cell lines (HOS and MG-63) and osteoblasts (hFOB) were purchased from the American Type Culture Collection. MG-63 and hFOB cells were cultured in DMEM (Gibco; Thermo Fisher Scientific, Inc.) supplemented with 10% fetal bovine serum (FBS; PAN-Biotech GmbH) and 100 U/ml penicillin/streptomycin in a humid atmosphere with 5% CO_2 at 37˚C. HOS cells were maintained in Eagle's Minimum Essential Medium containing 15% FBS (EMEM: Sigma-Aldrich; Merck KGaA) and 100 U/ml penicillin/streptomycin with 5% CO_2 at 37˚C in a humid atmosphere.

miR-487a mimic, mimic negative control (miR-NC), miR-487a inhibitor (50 nM), inhibitor scramble control (inhibitor-NC; all 50 nM), pcDNA (vector) and pcDNA-NKX3-1 overexpression (NKX3-1-OE) and pcDNA-KLF5 overexpression (KLF5-OE) plasmids were purchased from Shanghai GenePharma Co., Ltd. All transfections were performed using Lipofectamine® 3000 (Invitrogen; Thermo Fisher Scientific, Inc.) according to the manufacturer's instructions for 6 h in 37˚C. At 48 h post-transfection, cells were harvested for evaluation of transfection efficiency by reverse transcription-quantitative (RT-q)PCR analysis.

Western blotting. Proteins were extracted from HOS and MG63 cells using RIPA buffer (Beyotime Institute of Biotechnology; cat. no. P0013B) and the concentration of extracted protein was assessed by BCA kit (Thermo Fisher Scientific, Inc.). Protein was separated via 10% SDS-PAGE followed by transfer onto a polyvinylidene difluoride membrane. Membranes were blocked with 5% skimmed milk for 1 h at room temperature. The membranes were incubated with primary antibodies (GAPDH, 1:10,000, cat. no. ab181603; NKX3-1, 1:1,000, cat. no. ab196020; KLF5, 1:2,000, cat. no. ab137676; Abcam) overnight at 4˚C, followed by incubation with corresponding secondary antibodies (1:5,000; cat. no. 31430, HRP-conjugated, Thermo Fisher Scientific, Inc.) at room temperature for 2 h. Proteins bands were visualized using electrochemiluminescence (ECL Western Blotting Substrate; cat. no. 32106; Pierce; Thermo Fisher Scientific, Inc.) and analyzed using the ChemiDoc™ XRS Molecular Imager 3.0 system (Bio-Rad Laboratories, Inc.).

RT-qPCR. Total RNA was extracted from cells (HOS/MG63) using TRIzol® (Invitrogen; Thermo Fisher Scientific, Inc.). Extracted RNA was reverse transcribed to cDNA via cDNA RT kit (Roche Diagnostics GmbH) according to the manufacturer's instructions. RNA concentration was detected using Nanodrop (Invitrogen; Thermo Fisher Scientific, Inc.). RT-qPCR was performed using SYBR®Premix Ex Taq™ (Takara Bio, Inc.) with an ABI Prism 7900 Sequence detection system (Applied Biosystems; Thermo Fisher Scientific, Inc.). Thermocycling conditions of PCR cycling were as following: Activation of TaqMan at 95˚C for 10 min followed by 40 cycles of denaturation at 95˚C for 10 sec and annealing/extension at 60˚C for 60 sec. Primer sequences were synthesized by TsingKe Biological Technology (Table I). The relative expression of target genes was assessed via the $2^{-\Delta\Delta Cq}$ method (25). U6 and GAPDH were used as the internal controls. Each sample was tested in triplicate.

Luciferase reporter assay. StarBase 2.0 was used to predict the latent targeting association between miR-487a and NKX3-1, which was verified by luciferase reporter assay. HOS and MG-63 cells were transfected with pMIR-REPORT luciferase vector with wild-type (WT) or mutant (MUT)-NKX3-1-3'UTR (Promega) (1.6 ug per 12-well plate), miR-487a mimic, miR-487a inhibitor (miR-487a-KD) or miR-NC/inhibitor-NC using Lipofectamine 3000 (Invitrogen; Thermo Fisher Scientific, Inc.) as aforementioned. At 48 h post-transfection, luciferase activity was detected using Dual-Luciferase Reporter Assay System (Promega Corporation) according to the manufacturer's instructions. Renilla luciferase activity was used for normalization. Each assay was performed in triplicate.

Transwell assay. Cell invasion and migration were assessed using 6.5 mm Transwell® migration assay, with 8.0 μm Pore Polycarbonate Membrane Insert, Sterile (Corning, Inc.; cat. no. 3422). For cell invasion, serum-free medium was mixed with the BD Matrigel™ hESC-qualified Matrix (BD Biosciences; cat. no. 354277) in a 1:10 ratio. This mixture (50 μl) was added to the bottom of the insert. The Matrigel was then incubated at 37˚C for 4 h to solidify. Then, $5x10^4$ cells were transfected and at 24 h following transfection, cells were

Table I. Primer sequences for reverse transcription-quantitative PCR and oligonucleotides for miRNA mimic, inhibitor and negative control.

Primer	Sequence, 5'→3'
miR-487a	Forward: GCGGCGGAATCATACAGGGACATC
	Reverse: ATCCAGTGCAGGGTCCGAGG
U6	Forward: AACGCTTCACGAATTTGCGT
	Reverse: CTCGCTTCGGCAGCACA
GAPDH	Forward: CGGATTTGGTCGTATTGGG
	Reverse: TCTCGCTCCTGGAAGATGG
miR-219-5p	Forward: TGATTGTCCAAACGCAATTCT
	Reverse: ATCCAGTGCAGGGTCCGAGG
miR-331-5p	Forward: CTAGGTATGGTCCCAGGGATCC
	Reverse: ATCCAGTGCAGGGTCCGAGG
NKX3-1	Forward: GCCAAGAACCTCAAGCTCAC
	Reverse: AGAAGGCCTCCTCTTTCAGG
CDK6	Forward: TGCCCACTGAAACCATAAA
	Reverse: TACCACAGCGTGACGACCA
AJUBA	Forward: AGGCCAGGGAGGACTACTTCG
	Reverse: GCCTCCTGAAACCCTGAAA
DAPK1	Forward: AATCCTAGACGTGGTCCGGTAT
	Reverse: GTCCTCGGTGCGTATCCTTTCG
WNT5A	Forward: GCGAAGACAGGCATCAAAG
	Reverse: GCAAAGCGGTAGCCATAGTC
KLF5	Forward: ACACCAGACCGCAGCTCCA
	Reverse: TCCATTGCTGCTGTCTGATTTGTAG
KLF15	Forward: CAGCGGCAGTAGCATTGGG
	Reverse: ACCTCCTGCACTGGCACCAC
SP1	Forward: TGGTGGGCAGTATGTTGT
	Reverse: GCTATTGGCATTGGTGAA
SP4	Forward: ATGGCTACAGAAGGAGGGAAAAC
	Reverse: TTGACCAGGGGTGGAAGAATTAC
miR-487a mimic	Forward: GUGGUUAUCCCUGCUGUGUUCG
	Reverse: CGAACACAGCAGGGAUAACCAC
miR-NC	Forward: UUUGUACUACACAAAAGUACUG
	Reverse: CAGUACUUUUGUGUAGUACAAA
miR-487a-inhibitor	CGAACACAGCAGGGAUAACCAC
Inhibitor-NC	CAGUACUUUUGUGUAGUACAAA

miR, microRNA; NKX3-1, NK3 homeobox 1; AJUBA, ajuba LIM protein; DAPK1, death-associated protein kinase 1; KLF, Kruppel-like factor; SP, Sp transcription factor.

harvested by trypsinization, washed with serum-free medium (HOS: EMEM; MG63: DMEM) and placed in the upper chamber of the Transwell. The lower chamber contained 500 μl medium supplemented with 10% FBS that was used as chemo-attractant. After incubation at 37˚C with 5% CO_2 for 48 h, the cells in the inner side of the chamber were removed using cotton swabs. Invaded cells on the lower membrane surface were fixed with methanol for 15 min at room temperature and stained with 0.1% crystal violet for 10 min at room temperature. Images of the invaded cells were captured using a light microscope (Olympus IX71; x200 magnification) and cells were counted. Cell migration assay was performed in a similar way except that $1x10^5$ cells were added into the insert without Matrigel pre-coating. Each experiment was conducted in triplicate and repeated three times.

Cell viability assay. Viability of HOS and MG-63 cells was evaluated by MTT assay according to the manufacturer's instructions. In brief, cells were seeded into 96-well plates at a density of $2x10^3$ cells/well. Then, cells were incubated in a humid atmosphere with 5% CO_2 at 37˚C. MTT assay was performed after days 1-5. A total of 20 μl MTT (5 mg/ml) was added into each well followed by incubation for 4 h at 37˚C. Then, 100 μl dimethyl sulfoxide was added to dissolve the formazan crystals. Absorbance at 490 nm was detected with a microplate reader.

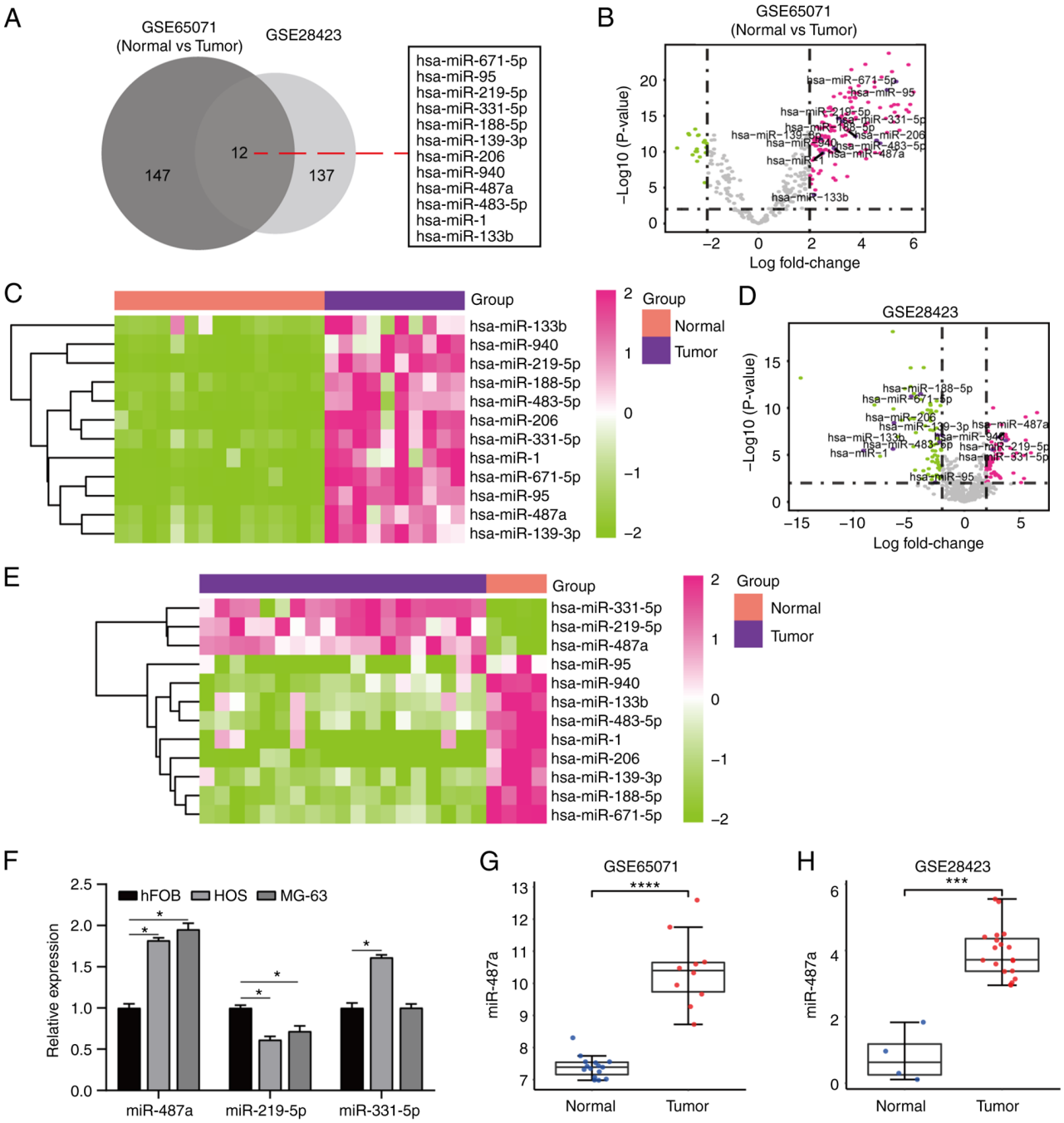

Figure 1. miR-487a expression is increased in OS. (A) A total of 12 DEMs between OS and non-OS tissue/cells was identified by overlapped analysis of miRs in GSE65071 and GSE28423 datasets. (B) Volcano plot and (C) heatmap of 12 DEMs observed in GSE65071 dataset. (D) Volcano plot and (E) heatmap of 12 DEMs in GSE28423 dataset. (F) reverse transcription-quantitative PCR analysis of miR-487a, miR-219-5p and miR-331-5p expression in HOS, MG-63 and hFOB cells. miR-487a expression in tumor and normal samples in (G) GSE65071 and (H) GSE28423 datasets. *P<0.05, ***P<0.001 and ****P<0.0001. miR, microRNA; DEM, differentially expressed miRNA; OS, osteosarcoma.

Colony formation assay. Transfected HOS and MG63 cells ($3x10^2$ cells/well) were digested with 0.25% trypsin to form a cell suspension, inoculated into 6-well plates and incubation at 37˚C in 5% CO_2 for 14 days. The cells were fixed with 70% ethanol at room temperature (20-25˚C) for 15 min and stained with 0.05% crystal violet at 37˚C for 20 min. The number of colonies formed was counted (≥50 cells) manually using an Olympus BX40 light microscope (Olympus Corporation).

Chromatin immunoprecipitation (ChIP) assay. According to the manufacturer's protocol, total genomic DNA was isolated using ChIP Assay kit (Beyotime Institute of Biotechnology; cat. no. P2078). A total of $2x10^6$ HOS/MG63 cells were transfected with pCDNA3.1 vectors and lysed with 250 μl SDS Lysis Buffer (Beyotime Institute of Biotechnology). Next, the HOS/MG63 cells were sonicated on ice and fragments of DNA were then resolved using a 2% agarose gel. For ChIP, samples were diluted in a 10X ChIP dilution buffer and pre-cleared with 60 μl protein G-agarose beads mixed at 4˚C for 1 h. During chromatin separation, the chromatin was centrifuged at 15,000 x g at 4˚C for 10 min to remove insoluble matter and then pre-cleared chromatin

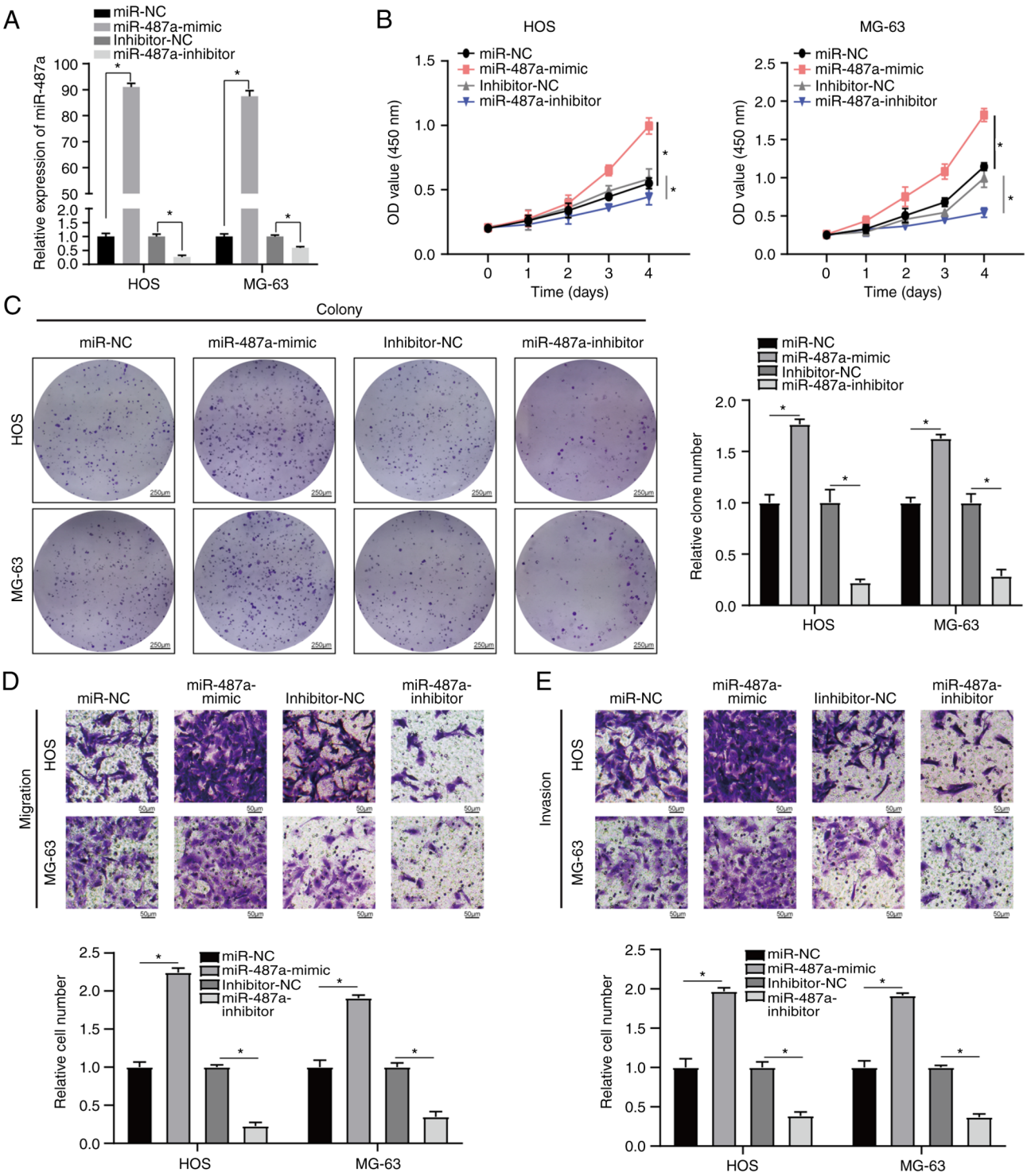

Figure 2. Effect of miR-487a on osteosarcoma cells *in vitro*. (A) Reverse transcription-quantitative PCR was used to assess miR-487a expression following transfection with miR-487a mimic or inhibitor in HOS and MG-63 cells. Proliferative capacity of osteosarcoma cells was tested by (B) cell viability and (C) colony formation assay following transfection with miR-487a mimic or inhibitor. Transwell assay was used to assess (D) migration and (E) invasion following transfection with miR-487a mimic or inhibitor in HOS and MG-63 cells. *P<0.05. miR, microRNA; NC, negative control; OD, optical density.

was incubated with 1 μl antibodies against KLF5 (dilution, 1:100; cat. no. ab137676; Abcam) at 4˚C overnight. The precipitates were washed with low-salt wash buffer, high-salt wash buffer and LiCI wash buffer, and rinsed with TE buffer twice. Immunochromatin was centrifuged at 15,000 x g for 10 min at 4˚C, boiled, and then was amplified via PCR as aforementioned.

Statistical analysis. The data are presented as the mean ± SD and were assessed via GraphPad Prism 7 (GraphPad Software, Inc.). Comparisons between two groups were performed by unpaired t test. Comparison between >2 groups were performed by one-way ANOVA followed by Tukey's post hoc test. All experiments were performed three times. P<0.05 was considered to indicate a statistically significant difference.

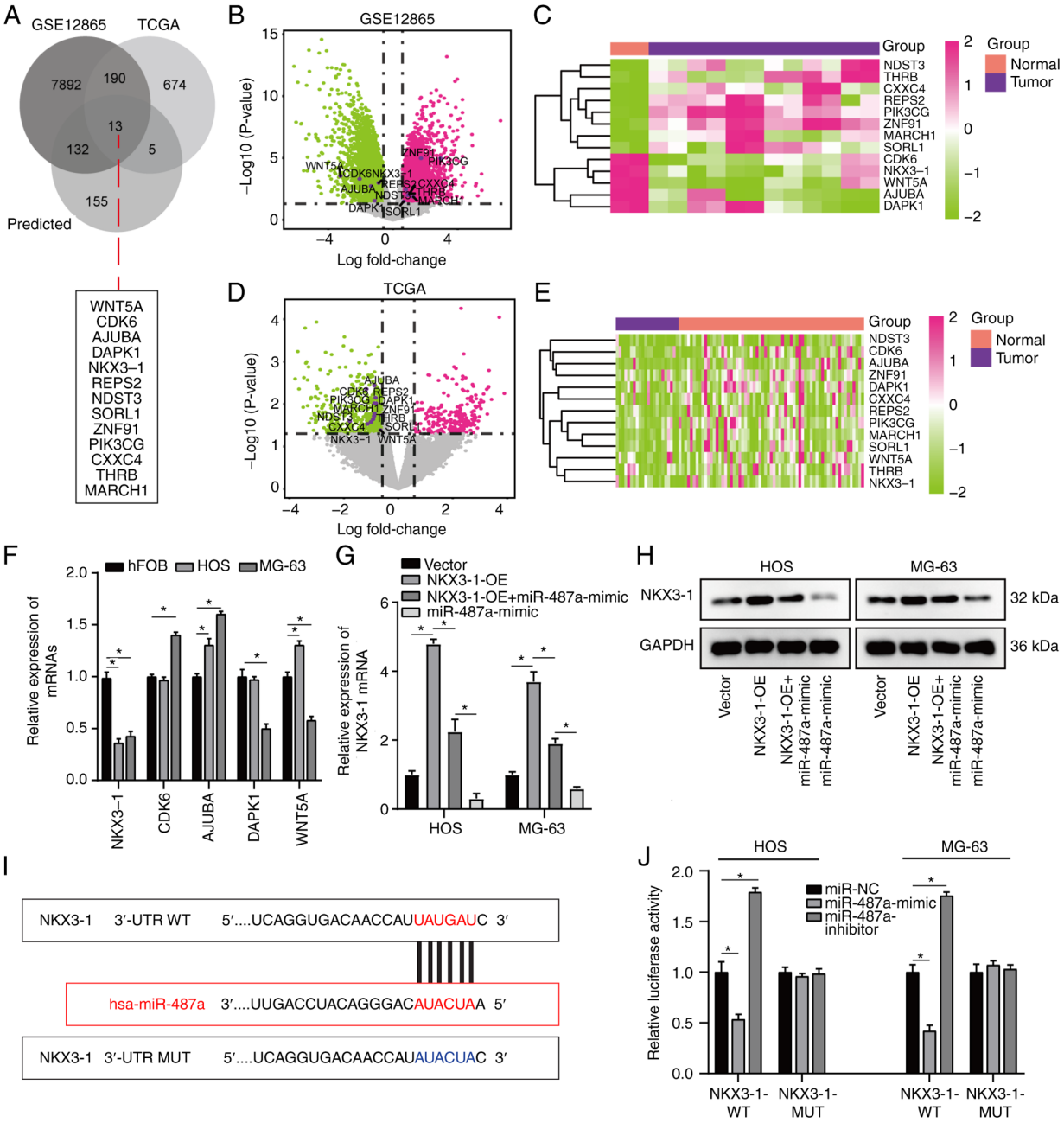

Figure 3. NKX3-1 is a direct target of miR-487a in osteosarcoma cells. (A) A total of 13 common target genes was identified by overlapping osteosarcoma DEGs between GSE12865 and TCGA and target genes predicted by miRWalk database. (B) Volcano plot and (C) heatmap of 13 DEGs in GSE12865 dataset. (D) Volcano plot and (E) heatmap of 13 DEGs in TCGA dataset. (F) RT-qPCR analysis of NKX3-1, CDK6, AJUBA, DAPK1 and WNT5A in HOS, MG-63 and hFOB cells. (G) Effect of miR-487a and NKX3-1-OE on NKX3-1 expression was assessed by RT-qPCR assay. (H) Western blot analysis of NKX3-1 following transfection with miR-487a mimic or inhibitor. (I) Binding site of miR-487a to NKX3-1 3'-UTR. (J) pMIR-REPORT luciferase vector containing WT or MUT NKX3-1 3'-UTR was co-transfected in HOS and MG-63 cells with miR-487a mimic, inhibitor or NC. Firefly luciferase activity was compared with *Renilla* luciferase activity. *P<0.05. NKX3-1, NK3 homeobox 1; miR, microRNA; DEG, differentially expressed gene; TCGA, The Cancer Genome Atlas; RT-q, reverse transcription-quantitative; AJUBA, ajuba LIM protein; DAPK1, death-associated protein kinase 1; WT, wild-type; MUT, mutant; UTR, untranslated region; NC, negative control; OE, overexpression.

Results

miR-487a expression is increased in osteosarcoma. Osteosarcoma DEMs were identified via overlapped analysis of osteosarcoma miRNAs in GSE65071 and GSE28423 datasets from GEO database (Table SI). A total of 12 DEMs was identified between osteosarcoma and non-osteosarcoma tissue (Fig. 1A) and volcano plot and heatmaps were constructed (Fig. 1B-E). RT-qPCR assay demonstrated that miR-487a was highly expressed in osteosarcoma (HOS and MG-63) compared with hFOB cells (Fig. 1F). miR-487a expression was significantly higher in tumor than in normal samples in GSE65071 and GSE28423 datasets (Fig. 1G and H). These results indicate that miR-487a was upregulated in osteosarcoma cells and tissue.

miR-143-5p promotes tumorigenesis of osteosarcoma cells. Osteosarcoma cells were transfected with miR-487a mimic or

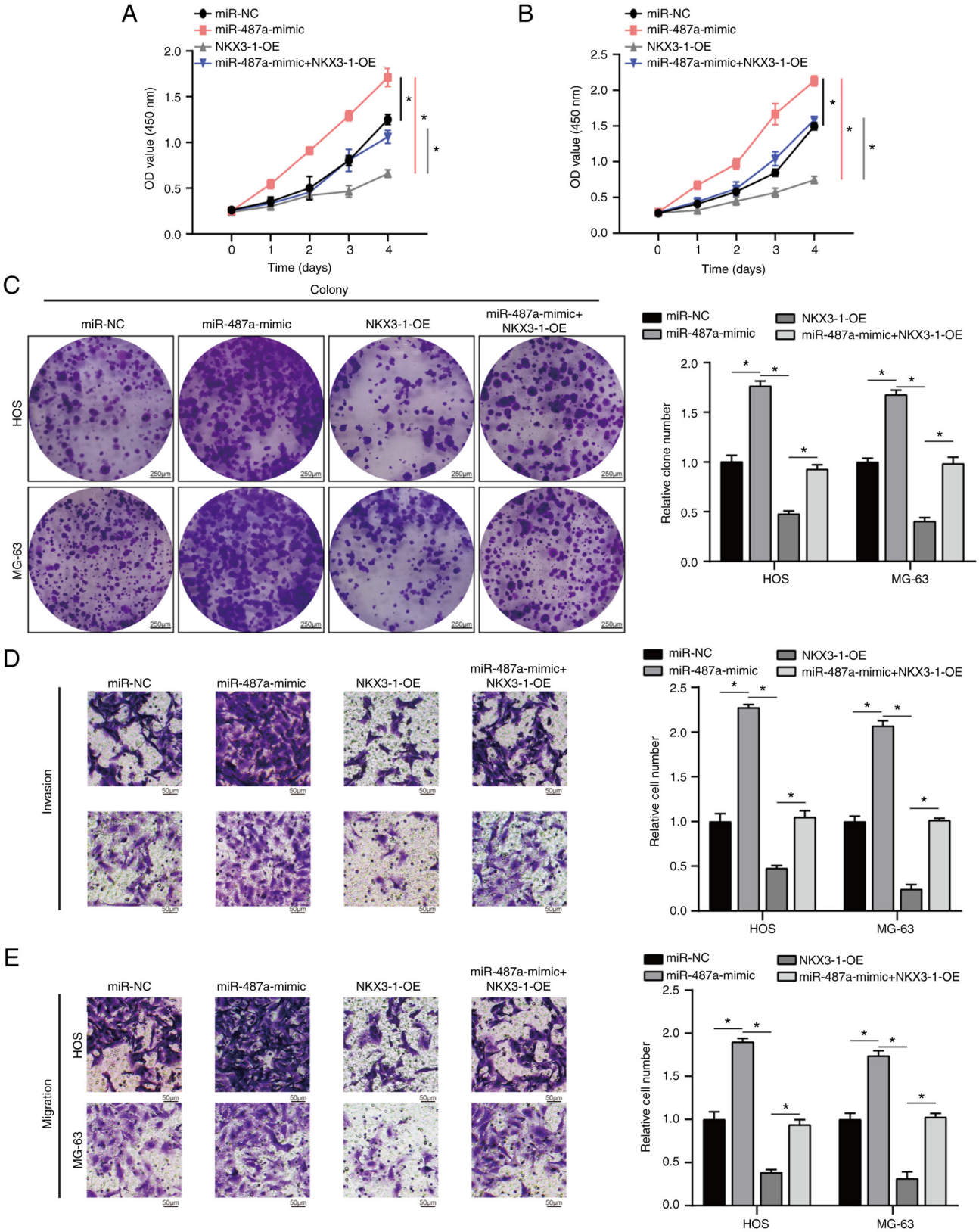

Figure 4. Overexpression of NKX3-1 rescues the effect of miR-487a on osteosarcoma cells. Effect of miR-487a and NKX3-1 on proliferation of (A) HOS and (B) MG-63 cells was detected by cell viability and (C) colony formation assay. Effect of miR-487a and NKX3-1 on (D) invasion and (E) migration of HOS and MG-63 cells was tested by Transwell assay. *P<0.05. NKX3-1, NK3 homeobox 1; miR, microRNA; OD, optical density; NC, negative control; OE, overexpression.

inhibitor. RT-qPCR indicated that miR-487a was significantly upregulated in osteosarcoma cells following transfection with miR-487a mimic compared with miR-NC and significantly downregulated following transfection with miR-487a inhibitor compared with inhibitor-NC (Fig. 2A). Transwell assay was used to assess the migratory and invasive capacity

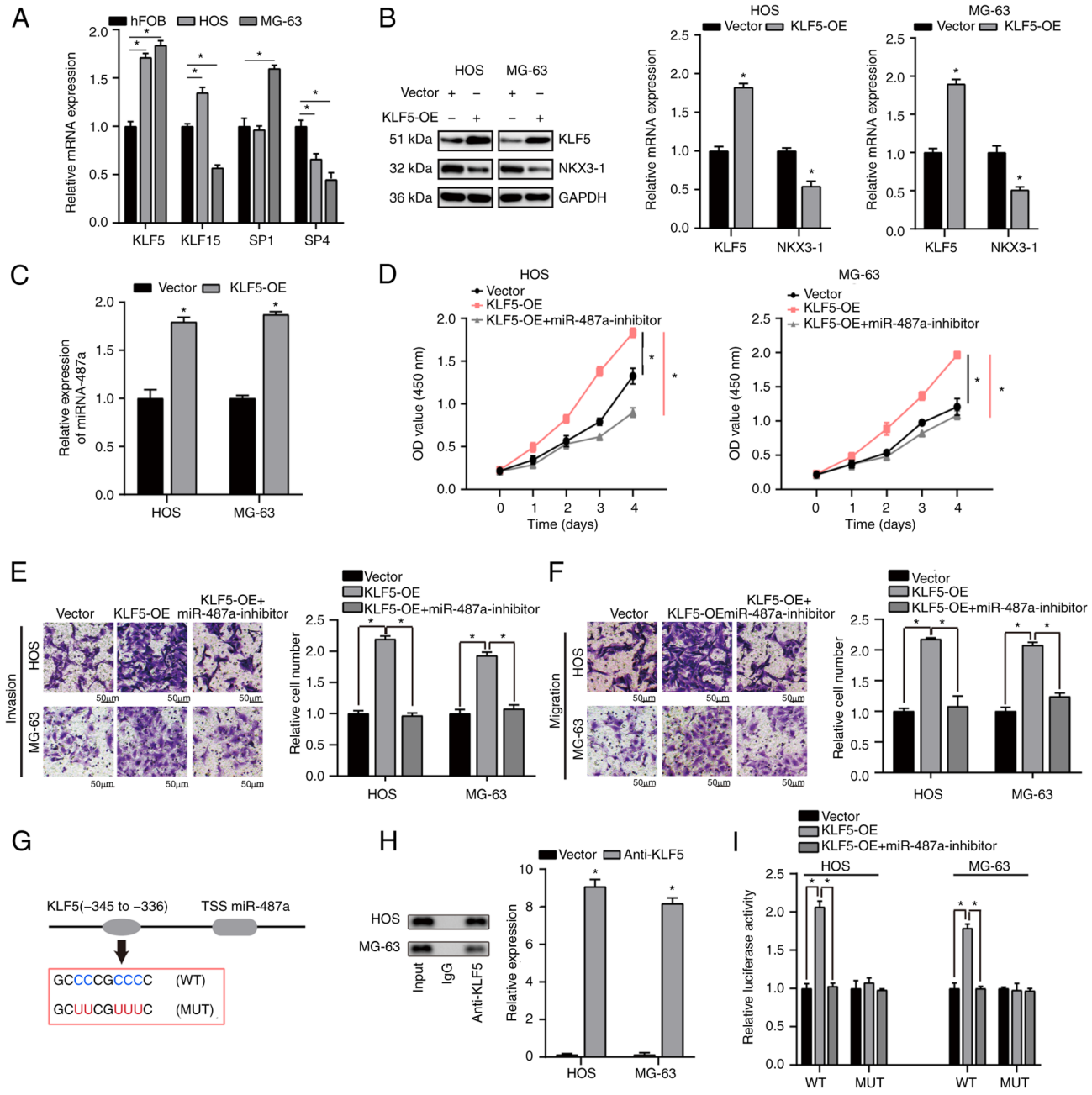

Figure 5. KLF5 directly regulates miR-487a expression in osteosarcoma cells. (A) RT-qPCR analysis of KLF5, KLF15, SP1 and SP4 expression. Effect of KLF5-OE on (B) NKX3-1 and (C) miR-487a in HOS and MG-63 cells was measured by western blot and RT-qPCR assay. (D) MTT assay showed KLF5-OE increased proliferative capacity of osteosarcoma cells; the effect was reversed by inhibited miR-487a expression. Transwell assay demonstrated that KLF5-OE significantly increased (E) invasion and (F) migration of HOS and MG-63 cells; this was rescued by miR-487a inhibition. (G) Proximal region of the miR-487a promoter. (H) Chromatin immunoprecipitation assay was performed to verify the binding site between KLF5 and miR-487a promoter in HOS and MG-63 cells. (I) Luciferase activity was increased following co-transfection with WT miR-487a promoter and KLF5-OE; this was significantly rescued by miR-487a inhibitor. No significant difference in luciferase activity was observed when KLF5 target sites at 336-345 bp were mutated. *P<0.05 KLF5, Kruppel-like factor 5; miR, microRNA; RT-q, reverse transcription-quantitative; SP, Sp transcription factor; OE, overexpression; NKX3-1, NK3 homeobox 1; WT, wild-type; MUT, mutant; TSS, transcription start site; OD, optical density.

of osteosarcoma cells. MTT assay was used to evaluate the proliferation ability of osteosarcoma cells. Overexpression of miR-487a significantly increased proliferation, invasion and migration of osteosarcoma cells. However, inhibition of miR-487a significantly decreased the proliferation, invasion and migration of osteosarcoma cells (Fig. 2B-E). Taken together, these data indicated that miR-487a promoted osteosarcoma progression via increased cell proliferation, invasion and migration.

NKX3-1 is a direct target of miR-487a in osteosarcoma cells and restoration of NKX3-1 rescues the effect of miR-487a. To analyze the effect of miR-487a on osteosarcoma cells, osteosarcoma DEGs between GSE12865 and TCGA database were overlapped (Table SI) and target genes were predicted using miRWalk database. A total of 13 common target genes were identified (Fig. 3A) and volcano plot and heatmaps were constructed for GSE12865 and TCGA database (Fig. 3B-E). Notably, five target genes (NKX3-1, CDK6,

AJUBA, DAPK1, WNT5A) were notably downregulated in both datasets (Fig. 3B-E). Of these five target genes, RT-qPCR demonstrated that NKX3-1 exhibited the lowest expression in osteosarcoma cells and was significantly decreased compared with its expression in hFOB cells (Fig. 3F). Additionally, the effect of miR-487a on NKX3-1 expression was assessed by RT-qPCR; expression of NKX3-1 was significantly decreased by transfection with miR-487a mimic in HOS and MG-63 cells (Fig. 3G). The effect of miR-487a on NKX3-1 was assessed via western blot analysis. miR-487a overexpression notably decreased expression levels of NKX3-1 in HOS and MG-63 cells (Fig. 3H). Online bioinformatics tool Starbase was used to search potential binding sites of miR-487a; NKX3-1 was predicted as a potential binding target of miR-487a (Fig. 3I). In addition, dual luciferase reporter assay indicated that luciferase activity was significantly decreased in osteosarcoma cells co-transfected with NKX3-1-WT-3'-UTR plasmid and miR-487a-mimic and significantly increased by co-transfection with miR-487a inhibitor (Fig. 3J), implying a direct regulatory association between miR-487a and 3'-UTR of NKX3-1 mRNA. In addition, miR-487a overexpression significantly increased proliferation, invasion and migration of HOS and MG-63 cells (Fig. 4A-E); these effects were significantly rescued by NKX3-1-OE. These data illustrated that overexpression of miR-487a exerted its role in HOS and MG63 cells by inhibiting NKX3-1.

KLF5 directly regulates miR-487a expression in osteosarcoma cells. To determine the upstream regulators of miR-487a, JASPAR database was used to determine the candidate transcription factors targeting promoters of miR-487a. RT-qPCR was used to measure the level of the top four transcription factors (KLF5, KLF15, SP1, SP4) that may directly regulate miR-487a expression. KLF5 was most highly expressed and was significantly upregulated in HOS and MG-63 compared with hFOB cells (Fig. 5A). Western blot analysis was used to assess KLF5 and NKX3-1 expression following transfection with KLF5-OE in HOS and MG-63 cells. NKX3-1 expression levels were significantly decreased following transfection with KLF5-OE in HOS and MG-63 cells compared with Vector (Fig. 5B). As demonstrated by RT-qPCR analysis, KLF5-OE significantly upregulated expression of miR-487a in HOS and MG-63 cells (Fig. 5C). KLF5-OE significantly promoted proliferation, invasion and migration of osteosarcoma cells; this effect was notably reversed by inhibition of miR-487a (Fig. 5D-F).

ChIP assay was used to determine whether KLF5 transcriptionally regulated miR-487a expression. Binding site of KLF5 in the miR-487a promoter region was identified using JASPAR database. ChIP assay identified the region-345 to -336 bp upstream of the pre-miR-487a promoter region as a target of KLF5 (Fig. 5G and H). Pre-miR-487a promoter region was present in the KLF5 fraction, which revealed that KLF5 may bind to miR-487a promoter region (Fig. 5H). Furthermore, luciferase activity of WT miR-487a promoter was significantly upregulated in HOS and MG-63 cells transfected with KLF5-OE compared with vector; the effect was significantly rescued by miR-487a inhibitor. No significant difference was found following mutation of KLF5 binding site 336-345 bp in upstream of the pre-miR-487a promoter region (Fig. 5I). These data suggested that KLF5-induced miR-487a promotes osteosarcoma progression via targeting NKX3-1.

Discussion

Recent evidence has illustrated that numerous miRNAs are dysregulated in osteosarcoma and serve as an oncogene or tumor suppressor (13,26). Here, miR-487a was significantly upregulated in osteosarcoma cells and tissue. However, the mechanism of miR-487a regulation of proliferation and metastasis in osteosarcoma remains unclear.

Here, miR-487a-OE markedly promoted proliferation, invasion and migration of HOS and MG-63 cells. miR-487a upregulation in cancer has been reported in multiple studies. For example, Chang *et al* demonstrated that miRNA-487a promotes proliferation and metastasis in hepatocellular carcinoma (27). Yang *et al* indicated that exosomal miR-487a derived from M2 macrophages promotes progression of gastric cancer (28); these data are consistent with the present results. NKX3-1 was predicted to be a direct target of miR-487a in osteosarcoma cells and confirmed by dual luciferase assay. In addition, the suppressive effect of NKX3-1 on proliferation, invasion and migration of HOS and MG-63 cells was confirmed. On the other hand, numerous studies have revealed that NKX3-1 serves as a tumor suppressor. For example, Jiang *et al* demonstrated that NKX3-1 increases forkhead box O1 expression in hepatocellular carcinoma, thereby suppressing tumor proliferation and invasion (29). Miyaguchi *et al* suggested that loss of NKX3-1 is a biomarker for poor prognosis in oral squamous cell carcinoma, which were consistent with the present study (30). The present results suggested that overexpression of miR-487a exert its role in osteosarcoma cells by inhibiting NKX3-1.

Other factors have been reported to be involved in the progression of osteosarcoma. For example, Ren and Gu revealed the prognostic implications of RB1 tumour suppressor gene alterations in the clinical outcome of human osteosarcoma (31). Li *et al* indicated that LINC01133 is an emerging tumor-associated long non-coding (lnc)RNA in tumor and osteosarcoma (32). Chen *et al* found that alkB homolog 5, RNA demethylase-mediated m(6)A demethylation of lncRNA PVT1 serves an oncogenic role in osteosarcoma (33). In addition, a previous study revealed that methyl 2-cyano-3,11-dioxo-18b-olean-1,12-dien-30-oate serves an antineoplastic role in bladder cancer cells by inducing ROS, which decreases Sp and Sp-regulated protein levels (34). The aforementioned study suggested that intracellular ROS serves an anti-tumor role in tumor. It was hypothesized that ROS may also serve a crucial role in development of osteosarcoma. Jia *et al* revealed that liensinine inhibits osteosarcoma growth by ROS-mediated suppression of the JAK2/STAT3 signaling pathway (35) and Rawat and Nayak (36) reported that Piperlongumine induces ROS-mediated apoptosis by transcriptional regulation of SMAD4/P21/P53 genes and synergizes with doxorubicin in osteosarcoma cells.

A recent study suggested that miR-487a serves an oncogenic role in osteosarcoma by targeting BTG2 mRNA (37). The present study also investigated the effect of miR-487a on osteosarcoma progression but focused on different target

genes and upstream transcription factors of miR-487a to identify novel drug targets for osteosarcoma. The present study combined bioinformatics with *in vitro* assays to identify up- and downstream regulatory molecules of miR-487a.

Numerous studies have revealed that transcription factors are associated with different types of cancer. For example, Zhao *et al* (38) found that activating transcription factor 3 mediates radioresistance of breast cancer. Zhu *et al* (39) indicated that KLF4 modulates miR-106a to target SMAD7 in gastric cancer. Huang *et al* (40) revealed that YY1 modulates lung cancer progression by activating lncRNA-PVT1. The present study predicted transcription factors that targeted the promoter of miR-487a using JASPAR database. KLF5 was identified as a key upstream regulator of miR-487a by RT-qPCR. The present study investigated the effect of KLF5-OE on miR-487a and NKX3-1 expression via RT-qPCR and western blot assay. The effect of KLF5-OE on osteosarcoma cell proliferation, invasion and migration was also investigated. A previous study revealed that KLF5 has a key effect on the microenvironment of cancer, which showed that high levels of M2 polarized macrophages is associated with upregulated KLF in bladder cancer and promotes angiogenesis, tumor grade and invasiveness (41). It was hypothesized that KLF5 may have a key effect on the microenvironment of osteosarcoma. Therefore, KLF5/miR-487a/NKX3-1 axis may serve a key role in the proliferation and progression of osteosarcoma, which may be a promising therapeutic target for osteosarcoma.

There are certain limitations to the present study. Firstly, the mechanism of KLF5 upregulation remains to be analyzed. In addition, other potential downstream target genes of miR-487a need to be investigated in the future.

The present study found that the KLF5/miR-487a/NKX3-1 axis played a significant role in proliferation, invasion and migration in osteosarcoma. Precision medicine may provide a more effective therapy strategy for patients with cancer based on individual variability. The present study suggested that the KLF5/miR-487a/NKX3-1 axis may serve as a therapeutic target for osteosarcoma. Inhibition of KLF5 and miR-487a and activation of NKX3-1 may exert a protective impact on osteosarcoma, which requires further investigation in future.

Acknowledgements

Not applicable.

Funding

No funding was received.

Availability of data and materials

The datasets used and/or analyzed during the current study are available from the corresponding author on reasonable request.

Authors' contributions

AL and CH confirm the authenticity of all the raw data. AL and HL collected data. AL and CH analyzed data and edited the manuscript. HL and CH performed the experiments and wrote the manuscript. All authors have read and approved the final version of the manuscript.

Ethics approval and consent to participate

Not applicable.

Patient consent for publication

Not applicable.

Competing interests

The authors declare that they have no competing interests.

References

1. Lindsey BA, Markel JE and Kleinerman ES: Osteosarcoma overview. Rheumatol Ther 4: 25-43, 2017.
2. Yang J and Zhang W: New molecular insights into osteosarcoma targeted therapy. Curr Opin Oncol 25: 398-406, 2013.
3. Ritter J and Bielack SS: Osteosarcoma. Ann Oncol 21 (Suppl 7): vii320-vii325, 2010.
4. Bernthal NM, Federman N, Eilber FR, Nelson SD, Eckardt JJ, Eilber FC and Tap WD: Long-term results (>25 years) of a randomized, prospective clinical trial evaluating chemotherapy in patients with high-grade, operable osteosarcoma. Cancer 118: 5888-5893, 2012.
5. Anderson ME: Update on survival in osteosarcoma. Orthop Clin North Am 47: 283-292, 2016.
6. Chu Y, Hu X, Wang G, Wang Z and Wang Y: Downregulation of miR-136 promotes the progression of osteosarcoma and is associated with the prognosis of patients with osteosarcoma. Oncol Lett 17: 5210-5218, 2019.
7. Wang H, Zhao F, Cai S and Pu Y: MiR-193a regulates chemoresistance of human osteosarcoma cells via repression of IRS2. J Bone Oncol 17: 100241, 2019.
8. Nishikawa R, Goto Y, Kurozumi A, Matsushita R, Enokida H, Kojima S, Naya Y, Nakagawa M, Ichikawa T and Seki N: MicroRNA-205 inhibits cancer cell migration and invasion via modulation of centromere protein F regulating pathways in prostate cancer. Int J Urol 22: 867-877, 2015.
9. Chen X and Zhang Y: BMP-2 and miR-29c in osteosarcoma tissues on proliferation and invasion of osteosarcoma cells. Oncol Lett 17: 5389-5394, 2019.
10. Chen T, Xu C, Chen J, Ding C, Xu Z, Li C and Zhao J: MicroRNA-203 inhibits cellular proliferation and invasion by targeting Bmi1 in non-small cell lung cancer. Oncol Lett 9: 2639-2646, 2015.
11. Qin C, Zhao Y, Gong C and Yang Z: MicroRNA-154/ADAM9 axis inhibits the proliferation, migration and invasion of breast cancer cells. Oncol Lett 14: 6969-6975, 2017.
12. Hannafon BN, Cai A, Calloway CL, Xu YF, Zhang R, Fung KM and Ding WQ: miR-23b and miR-27b are oncogenic microRNAs in breast cancer: Evidence from a CRISPR/Cas9 deletion study. BMC Cancer 19: 642, 2019.
13. Xia P, Gu R, Zhang W, Shao L, Li F, Wu C and Sun Y: MicroRNA-377 exerts a potent suppressive role in osteosarcoma through the involvement of the histone acetyltransferase 1-mediated Wnt axis. J Cell Physiol 234: 22787-22798, 2019.
14. Zhang G, Zhu Y, Jin C, Shi Q, An X, Song L, Gao F and Li S: CircRNA_0078767 promotes osteosarcoma progression by increasing CDK14 expression through sponging microRNA-330-3p. Chem Biol Interact 360: 109903, 2022.
15. Yang X, Wang M, Lin B, Yao D, Li J, Tang X, Li S, Liu Y, Xie R and Yu S: miR-487a promotes progression of gastric cancer by targeting TIA1. Biochimie 154: 119-126, 2018.
16. Ma M, He M, Jiang Q, Yan Y, Guan S, Zhang J, Yu Z, Chen Q, Sun M, Yao W, *et al*: MiR-487a promotes TGF-β1-induced EMT, the migration and invasion of breast cancer cells by directly targeting MAGI2. Int J Biol Sci 12: 397-408, 2016.
17. Li XL, Jones MF, Subramanian M and Lal A: Mutant p53 exerts oncogenic effects through microRNAs and their target gene networks. FEBS Lett 588: 2610-2615, 2014.

18. Liao JM, Cao B, Zhou X and Lu H: New insights into p53 functions through its target microRNAs. J Mol Cell Biol 6: 206-213, 2014.
19. Varet H, Brillet-Guéguen L, Coppée JY and Dillies MA: SARTools: A DESeq2- and EdgeR-based R pipeline for comprehensive differential analysis of RNA-Seq data. PLoS One 11: e0157022, 2016.
20. Castro-Mondragon JA, Riudavets-Puig R, Rauluseviciute I, Lemma RB, Turchi L, Blanc-Mathieu R, Lucas J, Boddie P, Khan A, Manosalva Pérez N, *et al*: JASPAR 2022: The 9th release of the open-access database of transcription factor binding profiles. Nucleic Acids Res 50 (D1): D165-D173, 2022.
21. Dweep H, Gretz N and Sticht C: miRWalk database for miRNA-target interactions. Methods Mol Biol 1182: 289-305, 2014.
22. Friedman RC, Farh KK, Burge CB and Bartel DP: Most mammalian mRNAs are conserved targets of microRNAs. Genome Res 19: 92-105, 2009.
23. Betel D, Koppal A, Agius P, Sander C and Leslie C: Comprehensive modeling of microRNA targets predicts functional non-conserved and non-canonical sites. Genome Biol 11: R90, 2010.
24. Kertesz M, Iovino N, Unnerstall U, Gaul U and Segal E: The role of site accessibility in microRNA target recognition. Nat Genet 39: 1278-1284, 2007.
25. Livak KJ and Schmittgen TD: Analysis of relative gene expression data using real-time quantitative PCR and the 2(-Delta Delta C(T)) method. Methods 25: 402-408, 2001.
26. Xu X and Liu M: miR-522 stimulates TGF-β/Smad signaling pathway and promotes osteosarcoma tumorigenesis by targeting PPM1A. J Cell Biochem 120: 18425-18434, 2019.
27. Chang RM, Xiao S, Lei X, Yang H, Fang F and Yang LY: miRNA-487a promotes proliferation and metastasis in hepatocellular carcinoma. Clin Cancer Res 23: 2593-2604, 2017.
28. Yang X, Cai S, Shu Y, Deng X, Zhang Y, He N, Wan L, Chen X, Qu Y and Yu S: Exosomal miR-487a derived from m2 macrophage promotes the progression of gastric cancer. Cell Cycle 20: 434-444, 2021.
29. Jiang J, Liu Z, Ge C, Chen C, Zhao F, Li H, Chen T, Yao M and Li J: NK3 homeobox 1 (NKX3.1) up-regulates forkhead box O1 expression in hepatocellular carcinoma and thereby suppresses tumor proliferation and invasion. J Biol Chem 292: 19146-19159, 2017.
30. Miyaguchi K, Uzawa N, Mogushi K, Takahashi K, Michikawa C, Nakata Y, Sumino J, Okada N, Mizushima H, Fukuoka Y and Tanaka H: Loss of NKX3-1 as a potential marker for an increased risk of occult lymph node metastasis and poor prognosis in oral squamous cell carcinoma. Int J Oncol 40: 1907-1914, 2012.
31. Ren W and Gu G: Prognostic implications of RB1 tumour suppressor gene alterations in the clinical outcome of human osteosarcoma: A meta-analysis. Eur J Cancer Care (Engl) 26, 2017.
32. Li Z, Xu D, Chen X, Li S, Chan MTV and Wu WKK: LINC01133: An emerging tumor-associated long non-coding RNA in tumor and osteosarcoma. Environ Sci Pollut Res Int 27: 32467-32473, 2020.
33. Chen S, Zhou L and Wang Y: ALKBH5-mediated m^6A demethylation of lncRNA PVT1 plays an oncogenic role in osteosarcoma. Cancer Cell Int 20: 34, 2020.
34. Takeuchi H, Taoka R, Mmeje CO, Jinesh GG, Safe S and Kamat AM: CDODA-Me decreases specificity protein transcription factors and induces apoptosis in bladder cancer cells through induction of reactive oxygen species. Urol Oncol 34: 337.e11-e18, 2016.
35. Jia F, Liu Y, Dou X, Du C, Mao T and Liu X: Liensinine inhibits osteosarcoma growth by ROS-mediated suppression of the JAK2/STAT3 signaling pathway. Oxid Med Cell Longev 2022: 8245614, 2022.
36. Rawat L and Nayak V: Piperlongumine induces ROS mediated apoptosis by transcriptional regulation of SMAD4/P21/P53 genes and synergizes with doxorubicin in osteosarcoma cells. Chem Biol Interact 354: 109832, 2022.
37. Gu Z, Wu S, Xu G, Wu W, Mao B and Zhao S: miR-487a performs oncogenic functions in osteosarcoma by targeting BTG2 mRNA. Acta Biochim Biophys Sin (Shanghai) 52: 631-637, 2020.
38. Zhao W, Sun M, Li S, Chen Z and Geng D: Transcription factor ATF3 mediates the radioresistance of breast cancer. J Cell Mol Med 22: 4664-4675, 2018.
39. Zhu M, Zhang N and He S: Transcription factor KLF4 modulates microRNA-106a that targets Smad7 in gastric cancer. Pathol Res Pract 215: 152467, 2019.
40. Huang T, Wang G, Yang L, Peng B, Wen Y, Ding G and Wang Z: Transcription factor YY1 modulates lung cancer progression by activating lncRNA-PVT1. DNA Cell Biol 36: 947-958, 2017.
41. Takeuchi H, Tanaka M, Tanaka A, Tsunemi A and Yamamoto H: Predominance of M2-polarized macrophages in bladder cancer affects angiogenesis, tumor grade and invasiveness. Oncol Lett 11: 3403-3408, 2016.